A MULTIPHASE FLOW MODEL IN A DISCRETE FRACTURE NETWORK: FORMULATION AND SIMULATION EXAMPLE

C. BAUJARD✉ and D. BRUEL

Gentre d'Informatique Géologique, ENSMP,
35 rue Saint Honoré, F-77305 Fontainebleau Gedex, France
E-mails: clement.bauj ard@ensmp.fr, dominique.bruel@ensmp.fr

Abstract

A two-phase flow in a discrete fracture network numerical model is presented to simulate the behaviour of any fractured aquifer. The purpose of this work is to consider density-driven flows induced by the density difference between two non-miscible fluids. Mechanical consequences of high pressure waves on fracture permeability and heat exchanges between fluids and rock matrix are not explained here. We describe the formulation of the flow problem, the assumptions that are made and the spatial discretisation method used, that is a finite volume method. The system is solved with an IMPES scheme, and equations linearised with the Newton-Raphson algorithm. The well-known Buckley-Leverett example is then adapted to this approach of reservoir modelling and examinated in order to validate the results obtained wilth this new code. The example of a salt intrusion in a fractured coastal aquifer is then treated; it consists in the calculation of the localization of the interface between sea water and fresh water in steady state. To conclude, recent results accounting for some additional hydro-mechanical couplings are shown. The simulation example of the hydraulic behaviour of a geothermal reservoir located in Soultz-sous-Forets, France is discussed.

Keywords: Multiphase flow, fracture network, IMPES, Buckley-Leverett, coastal aquifer, geothermal energy.

Introduction

The general background of this note is the European Hot Dry Rock Research Program located in Soultz-sous-Forets, France. The purpose of this program is to generate electrical power from a deep enhanced geothermal system. The idea consists in injecting cold water into a hole while producing hot water in adjacent ones. The first step of this geothermal exploitation of the subsurface is the development

✉ Corresponding author

of the reservoir, released by very high pressure injections in the system. The role of these injections is to enhance the permeability of the fractures by increasing the water pressure until shear can develop along the fractures. The injected fluid is essentially cold, fresh water that will be in contact in the reservoir with hot rocks and heavy hot brines.

The model presented here has been written in order to simulate eventual density driven flows during stimulation of the reservoir, occuring between brine and fresh water. It is based on the Discrete Fracture Network approach; flows in the rock matrix are neglected. Fractures are considered as discs: their distribution in space, orientation and thickness respond to stochastic laws infered from the available statistics. The continuity equation is written at the center of each fracture. Each center of a fracture is a node of the mesh, and the controlled volume of each node is the fracture volume.

This paper describes the mathematical model, the spatial discretisation used, the resolution of the nonlinear system, a validation of the model, with the BuckleyLeverett problem and two examples of application of this code.

Equations used come from the continuity equation of each phase; many authors describe them (Huyakorn and Pinder 1983; Slough *et al.* 1999). The spatial discretisation is done after a finite volume scheme, and the evaluation of fluxes between two connected nodes consider the geometry of intersection of the two fractures (Cacas 1989; Jeong 2000). The system is solved with an IMPES scheme for Implicit Pressure - Explicit Saturation (Coats 2000; Forsyth *et al.* 1997); this technique is explained below 2. It consists in resolving implicitly a single pressure equation, and explicitly a saturation equation, using the computed pressure values.

The Buckley-Leverett test case, commonly used in the petroleum industry is used as a numerical benchmark. Briefly, it simulates the advancement of a saturation front in a porous media. Computed results can be compared with results of the analitycal solution written by Buckley and Leverett (1946). This test example is also developed and discussed below 3. To conclude, two examples of simulation are shortly exposed. The first one shows the establishment of a steady state flow in a coastal aquifer. The last one gives simulation results obtained with a discrete fracture network of the Soultz-sous-Forets research site (Bruel 2003).

Numerical formulation

Governing equations

The equations describing a two-phase flow are obtained by combining Darcy's law with the individual phase conservation. They may be written in the following form (Huyakorn *et al.* 1994):

$$\nabla.\left(k\tau^l\nabla(P^l+\rho^l gz)\right)=\frac{\partial}{\partial t}(\rho^l\Phi S^l)-M_l, \qquad (1)$$

where subscript l denotes the phase; k is the intrinsic permeability; τ^l is the mobility of the phase l ($\tau^l = k_r{}^l\rho^l/\mu^l$,in which $k_r{}^l$ is the relative permeability, ρ^l is the fluid density and μ^l is the fluid dynamic viscosity);

t is time; ρ^l is the pressure of the phase l; g is the gravitatiounal acceleration; z is the elevation above the datum plane; Φ is the porosity; S^l is the saturation of the phase l; M^l is the rate of mass injection or withdrawal of fluid phase l per unit volume of the medium.

In addition to these flow equations, the following constitutive relations have to be considered, being P the average pressure of the two fluids:

$$S^{l_1} + S^{l_2} = 1 \tag{2}$$

$$k_r^l = k_r^l(S^l) \tag{3}$$

$$k = k(e) \tag{4}$$

with e being the aperture of the considered fracture. A cubic law is generally used to describe the dependency of k with e (Marsily 1981). However, a strong non-linearity may appear here, as the aperture of the fractures becomes stress dependant at great depth (Gentier 1986), and therefore k may also depend on the pressure. This coupling is not described here as it does not form the main subject of this paper.

Major assumptions

The Boussinesq assumption

The Boussinesq assumption is quite common in reservoir modelling; it consists in neglecting any variations of the fluid densities in equation (1), except in the baoyancy term ($P^l + \rho^l gz$) (Helmig 1997). Equation (1) now becomes:

$$\nabla . \left(k \frac{k_r^l}{\mu^l} \nabla (P^l + \rho^l g z) \right) = \frac{\partial}{\partial t} (\Phi S^l) - Q^l, \tag{5}$$

where Q^l *is* the volumic rate of injection or withdrawal of fluid phase l per unit volume of the medium.

The zero-capillary pressure assumption

The capillary pressure is often neglected in reservoir modelling because it is usually very small compared to pressure variations in subsurface flows (Helmig 1997).

Practically, this leads us to:

$$P^{l_1} = P^{l_2} = P \tag{6}$$

Numerical treatment

The numerical method used is very classical; it consists in a finite volume discretisation, associated with an IMPES resolution scheme.

Finite volume spatial discretisation

The finite volume method is a well-established method that is used in porous media. Our purpose is to adapt this method to a discrete network of fractures. This can be done thanks to the physical aspect of the finite volume formulation.

This formulation is obtained by integrating the conservation equation (5) over the volume V_{frac} of one fracture:

$$\int_{V_{frac}} \nabla.\left(k\frac{k_r^l}{\mu^l}\nabla(P+\rho^l gz)\right)dV = \int_{V_{frac}} \frac{\partial}{\partial t}(\Phi S^l)\,dV - \int_{V_{frac}} Q^l dV \tag{7}$$

At that point we must underline that Φ no longer is the porosity of an equivalent porous media but it is the porosity of the considered fracture.

Applying the divergence theorem to the last equation, and making the assumption that saturation and porosity are constant in a single fracture, one obtains:

$$\int_{S_{int}} k\frac{k_r^l}{\mu^l}\nabla(P+\rho^l gz).\vec{n}\,dS = V_{frac}\frac{\partial}{\partial t}(\Phi S^l) - q^l, \tag{8}$$

where q^l *is* the rate of injection or withdrawal of the fluid *l*, S_{int} is the surface of the intersection between neighbouring fractures and $\vec{n}$ is a unit vector, normal to the surface of intersection of two fractures and pointing outside of the considered fracture.

Physically, the left term of equation (8) is the flow going out of the considered fracture through an adjacent one. In our code this term is computed using an "integrated intrinsic permeability", k_{ij}^{int}, calculated for the link between fractures i and j as follows:

$$k_{ij}^{int} = \frac{k_i.k_j}{k_i+k_j}.S_{int}(fracture\ i, fracture\ j) \tag{9}$$

Then, making the assumption that pressure is constant over one fracture and developing the gradient term to the first order, equation (8), written for the fracture i becomes:

$$\sum_j k_{ij}^{int}\frac{k_r^l(S_{ij}^l)}{\mu^l}\left(\frac{(P_i+\rho^l gz_i)-(P_j+\rho^l gz_j)}{\Delta x_{ij}}\right) = V_i\frac{\partial}{\partial t}(\Phi_i S_i^l) - q^l, \tag{10}$$

using an upstream weighting scheme for the calculation of relative permeabilities:

$$S_{ij}^l = \alpha S_i + (1-\alpha)S_j \tag{11}$$

with $\alpha = 1$ if $P_i + \rho^l gz_i > P_j + \rho^l gz_i$ and $\alpha = 0$ if not.

The IMPES scheme

Solving such a system of equations is not easy; as underlined by Peaceman (1977) the problem is parabolic in pressure and hyperbolic in saturation. Using a finite volume formulation provides, and that is important,

numerical stability to the computation method. The IMPES method consists in solving implicitly the pressure equation and in solving explicitly the saturation equation, with the computed pressure values. The basic idea is to obtain a single pressure equation by summing the flow equations (Settari and Aziz 1990). As $S^{l_1} + S^{l_2} = 1$, one obtains:

$$\sum_j \left(k_{ij}^{int} \frac{k_r^{l_1}}{\mu^{l_1}} + k_{ij}^{int} \frac{k_r^{l_2}}{\mu^{l_2}} \right) \left(\frac{P_i - P_j}{\Delta x_{ij}} \right) = V_i \frac{\partial \Phi_i}{\partial t} - \tag{12}$$

with

$$A_i = q^{l_1} + q^{l_2} + \sum_j k_{ij}^{int} \left[\frac{k_r^{l_1}}{\mu^{l_1}} \left(\frac{\rho^{l_1} g z_i - \rho^{l_1} g z_j}{\Delta x_{ij}} \right) - \frac{k_r^{l_2}}{\mu^{l_2}} \left(\frac{\rho^{l_2} g z_i - \rho^{l_2} g z_j}{\Delta x_{ij}} \right) \right] \tag{13}$$

The transient term of equation (12) can be written, using Euler's implicit temporal discretisation scheme:

$$V_i \frac{\partial \Phi_i}{\partial t} = V_i \frac{\partial \Phi_i}{\partial P_i} \frac{\partial P_i}{\partial t} = V_i C_i \frac{\partial P_i}{\partial t} = V_i C_i \frac{P_i^{t+\Delta t} - P_i^t}{\Delta t}, \tag{14}$$

where C_i is the storage coefficient of the fracture i per unit volume.

Equation (12) is solved using the Newton-Raphson's algorithm because of the strong non-linearity of $k_{ij}^{int}(P_i, p_j)$; the saturations are oLtained by replacing $P^{t+\Delta t}$ into one of the flow equations, assumming that Φ is constant:

$$S_i^{t+\Delta t} = S_i^t - \frac{\Delta t}{V_i \Phi_i} \sum_j k_{ij}^{int} \frac{k_r^l}{\mu^l} \left(\frac{(P_i + \rho^l g z_i) - (P_j + \rho^l g z_j)}{\Delta x_{ij}} \right) \tag{15}$$

Test case: the Buckley-Leverett problem

This test problem is a very classical numerical benchmark for simulation codes in reservoir modelling. More precisely, it is a one dimensional flow problem, that was first solved by Buckley and Leverett (1946), since then it has been used by many scientists in order to evaluate the behaviour of their codes (Settari and Aziz 1990; Huyakorn and Pinder 1978).

Physical parameters

The Buckley-Leverett problem consists in injecting a fluid at one side of a onedimensional porous media while extracting the inital fluid at the other side of it (see Figure 1). The geologic media and both fluids are assumed to be incompressible, and capillary pressure is neglected. A moving saturation front between the two fluids is observed; its shape and its migration rate are a severe test for numerical models. As pointed out by Buckley and Leverett (1946), the shape of the front strongly depends on the relative permeabilities. The analytical solution, obtained by the characteristics method, won't be explained here. Please refer to Dahle, Espedal, Ewing, and Saevareid (1990) for further information.

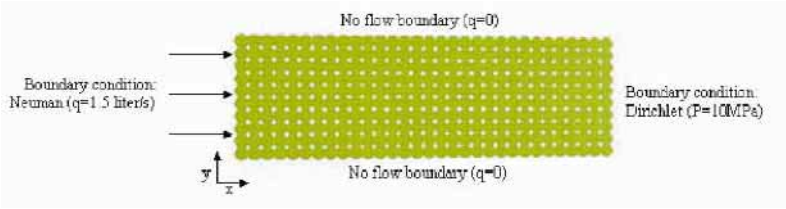

Figure 1. Geometry for the Buckley-Leverett problem.

The difficulty is to adapt this example from a porous media to a discrete fracture network. Two ways of proceeding are possible: building a stochastic network and deduce its equivalent permeabilities and porosity, or working on a deterministic network, like a plane, built by juxtaposition of fractures. This method appeared to be easier to perform. Nodes of the mesh are at the center of the fractures, every 10 meters. In order to fit to a finite difference scheme, the radius of the fractures is set to 5.64 m. Using this value, the area of one fracture is equal to the area of one mesh, which means that the porosity of the network is equal to the porosity of a single fracture. This fracture network is equivalent to a porous media of a cross section of 10^{-1} m^2

Table 1 shows the physical parameters used to compute the BuckleyLeverett solution. As it can be seen on this table, the equivalent area of cross section of our model is 10^{-1} m; implying a Darcy velocity of 1.5 10^{-2} m/s. It means that the simulation duration of 1296 s is equivalent to an ellapsed time of 1500 days following the values used by Thorenz (2001).

Table 1. Parameters used in the Buciley-Leverett example.

Physical parameter	Used value	Value in Thorenz (2001)
Lengh	$300\,m$	$301.95\,m$
Width	$100\,m$	$1\,m$
Height	-	$10\,m$
Thickness of the fractures	$10^{-3}\,m$	-
Simulation time	$1296\,s$	$969\,days$
Porosity	0.2	0.2
Permeability	$1\ 10^{-8}\,m/s$	No influence
Relative permeability	$k_r^l = \left(\frac{S^l - 0.2}{0.6}\right)^2$	$k_r^l = \left(\frac{S^l - 0.2}{0.6}\right)^2$
Viscosity	$1000\,Pa.s$	$1000\,Pa.s$
Injection rate	$1.5\ 10^{-3}\,m^3/s$	$1.5\ 10^{-6}\,m^3/s$
Initial saturation	0.2	0.2
Saturation of the injected fluid	0.8	0.8

Results

Figure 2 is a cross section of the model along the x axis and shows the advancement and the shape of the saturation front at a time of 1296 s. The time stop of this simulation is set to 20 s, and the mesh size is set to 10 m. The theoretical front was established with the characteristic method. The mass balance is good, as the areas delimited by the two curves are equal.

The shape of the computed front is acceptable as the shock wave is not damaged too much by numerical diffusion. One can observe a small difference between the two profiles. It is due to the inability of the finite volume method to capture sharp fronts. As underlined by Faust (1985), this kind of difficulties is very usual in reservoir simulation. Thorenz (2001) proposed numerical methods in order to skip this problem *(mass lumping* and *Gaussian point upwinding),* but none of them could be applied to a finite-volume numerical scheme.

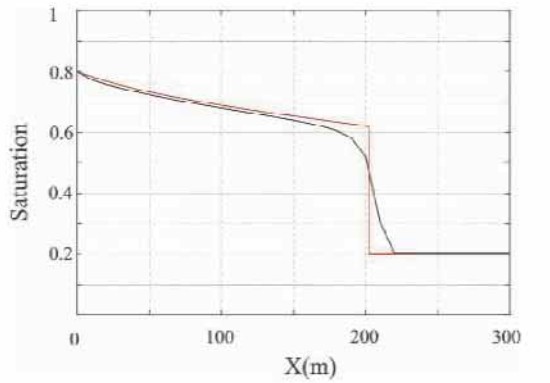

Figure 2. Results for the Buckley-Leverett problem (Δx = 10 m). See Table 1 for physical parameters.

A second simulation was made in order to enhance results presented in Figure 2. To reduce the numerical diffusion, the mesh size was reduced to 5 m (radius of fractures 2.32 m), and the time step remained unchanged. Results are presented in Figure 3.

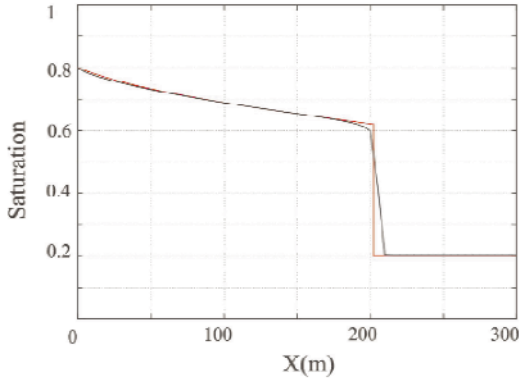

Figure 3. Results for the Buckley-Leverett problem (Δx = 5 m). See Table 1 for physical parameters.

Application examples

The purpose of this section is to give the reader an idea of the results that can expected with this multiphase flow simulation code. The first of these test cases describes a system where the fluids differ by their densities. No other coupling is involved. In the second application, some hydromechanical interactions can develop according to pressure changes in the reservoir.

Application to a coastal aquifer

Geometry of the model

As a first example of the capabilities of our code, we simulated a salt water intrusion into a network of fractures that is representing a coastal aquifer (see Figure 4).

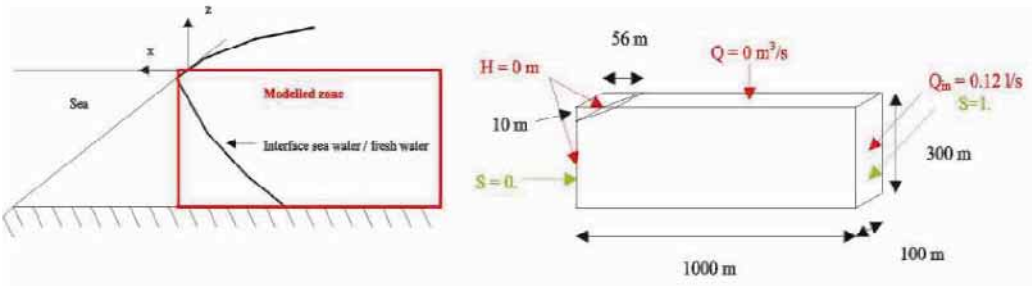

Figure 4. Geometry of the coastal aquifer model.

The left side of the model is a contact area with the sea (ρ_s = 1.025). The right vertical boundary is an inflow surface of fresh water (ρ_w = 1). The model is initially filled in with fresh water and the purpose of the simulation is to reach a steady-state flow situation. About 15.000 fractures compose this model and their orientation are very strictly equally distributed in space in order to get an isotropic permeability. The average fracture radius is 12.5 m and the total volume density of fractures is 3 10^{-4} m^{-3}

Results

Figure 5 shows the fresh water hydraulic head distribution in the model after 100 days of simulation (the steady-state flow is reached).

Because of the inflow imposed on the right limit of the model, the hydraulic head (initially equal to zero) increase to a value of about 7.5 m. As one can observe on this image, the Ghyben-Herzberg assumption (equipotential lines are vertical) is quite true in the upper right quarter of the model. Another simulation was done with the same fracture network but with only one fluid (fresh water) without the upper discharge surface in order to compute the upscaled permeability of this network. Knowing the prescribed flow rate, the section of the model and the resulting hydraulic head distribution (that is linear along the x-axis), a basic application of the Darcy's law can give this permeability. This network gave us a permeability K of 1.2 10^{-6} m/s.

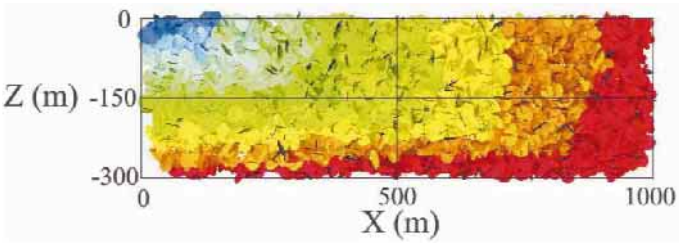

Figure 5. Fresh water hydraulic head distribution (t = 100 days). Dark blue on the upper left corner: 0 m; dark red (lower right corner): 7 m.

With that permeability, we could then calculate the equation of the Verruijt flow line (Marsily 1981) that gives the limit of a salt water intrusion into a coastal aquifer:

$$z^2 = -\frac{2Q}{\beta K(1+\beta)}x + \frac{Q^2}{\beta^2 K^2}\frac{1-\beta}{1+\beta} \tag{16}$$

where Q is the flow rate of fresh water per unit widht, K is the intrinsic permeability of the aquifer, and $\beta = \frac{\rho_s - \rho_w}{\rho_w} \simeq 0.025$.

Figure 6 shows the results of the simulation in terms of saturation, and the Verruijt flow line is superimposed.

The Verruijt flow line is quite close to the limit our model tend to, but we can observe a lens of fresh water in the salt water and a lens of salt water in the fresh water. Although numerical instabilities are not totally discarded, we suspect that this is due to preferential flow lines in the fracture network and to badly connected fractures that cannot be emptied once they are filled.

This first application using a random fracture network is quite successful and allows us to perform with confidence other tests implying more complex couplings.

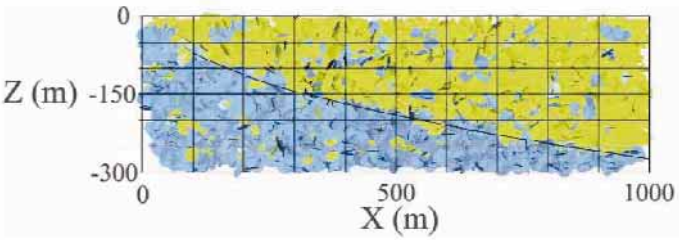

Figure 6. Saturation distribution (t = 100 days). In blue: salt water; in green: fresh water. (below the line).

Application to the Soultz-sous-Forets fracture network

This simulation has been computed after a fracture network model of the Soultzsous-Forets research site was built a few months ago (Bruel 2003).

The model

Figure 7 shows the geometry of the fracture network used to simulate the behaviour of the geothermal reservoir of Soultz. Nearly 45.000 fractures (represented as connected disks on the picture) compose this model; they belong to five different sets of fractures. Their positions, orientations, thicknesses and radii respond to stochastic laws. On this figure, one quarter of the fractures have been removed in order to see the propagation of the saturation front near the injection well, named GPK3.

The block dimensions are 3 km in the North-South direction and 2 km in the EstWest and vertical direction. The base of this network is located at 5 km in depth. The network is elongated in the N160E direction, highly dipping to the west. The width of the fractured reservoir is about 400 m, as derived from in situ microseismicity generation during injection tests. On a numerical point of view, this application differs from the two previous ones by a mechanical coupling that appears in the calculation of the intrinsic permeability; a normal compliance is introduced and the aperture now depends on effective normal stress, according to a hyperbolic closure law (Bandis *et al.* 1960).

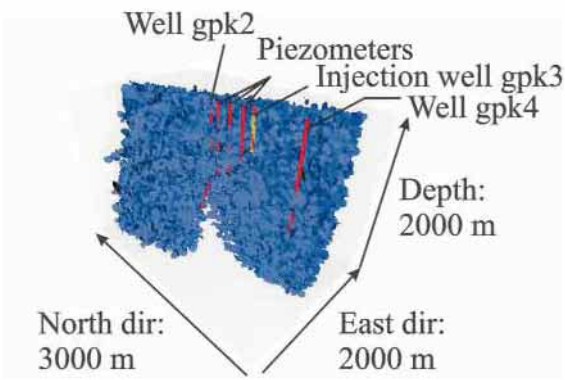

Figure 7. 3D view of the geometry of the Soultz-sous-Forêts fracture network.

Results

Two different simulations have been performed with this model. Both of them consist in injecting a fluid into reservoir filled in with a "natural" fluid at a rate of 25 l/s during two days. Relative permeabilities linearily depend on saturation for both simulations. The only difference between the two simuations concerns the density of the fluids. In the first one, both fluid have the same density (equal to 1000 kg/m^3), whereas in the second one, the injected fluid (ρ = 1100 kg/m^3) is heavier than the autochtonous one (ρ = 1060 kg/m^3).

The figures 8 and 9 show the advancement of the saturation front at the end of the two days of injection. As one can see, no significant differences are observed between these pictures; the simulation time of two days is too short to observe important density driven flows that could be seen on these images. May be different relative permeabilies should leed to more different results.

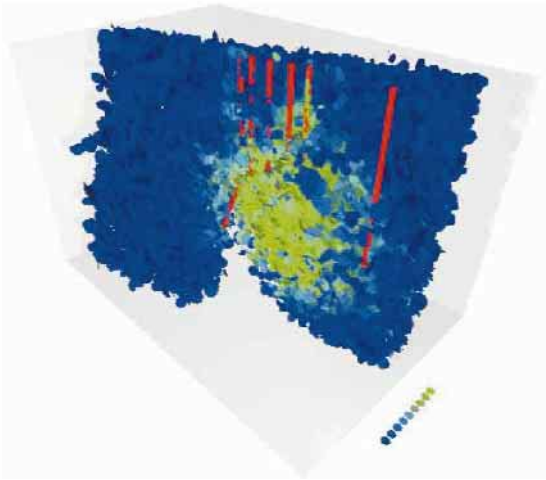

Figure 8. Fluid distribution at the end of the first simulation. In dark (blue): autochtonous fluid (Saturation=0.); in clear (green): injected fresh water (Saturation=1).

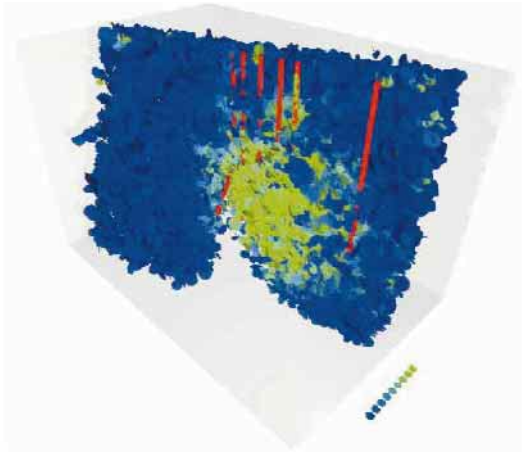

Figure 9. Fluid distribution at the end of the second simulation. In dark (blue): autoctonous fluid (Saturation=0.); in clear (green): injected fresh water (Saturation=1.).

Figures 10 and 11 show the calculated pressure and saturation in the wells and piezometers for each example.

Two observations can be made on these graphs. The first one is that the calculated pressure is higher in the second simulation than in the first one. This is due to the higher density of the autochtonous fluid in this example. The second observation consists in the speed of propagation of the saturation front; it seems to be higher in the second example. This may be due to an important connectivity of fractures to piezometers in the lowest part of the piezometers. Heavier fluid has a tendency to go in the lowest part of the reservoir. The consequence of this density driven flow is a higher saturation in piezometers, that catch fractures of the bottom of the reservoir.

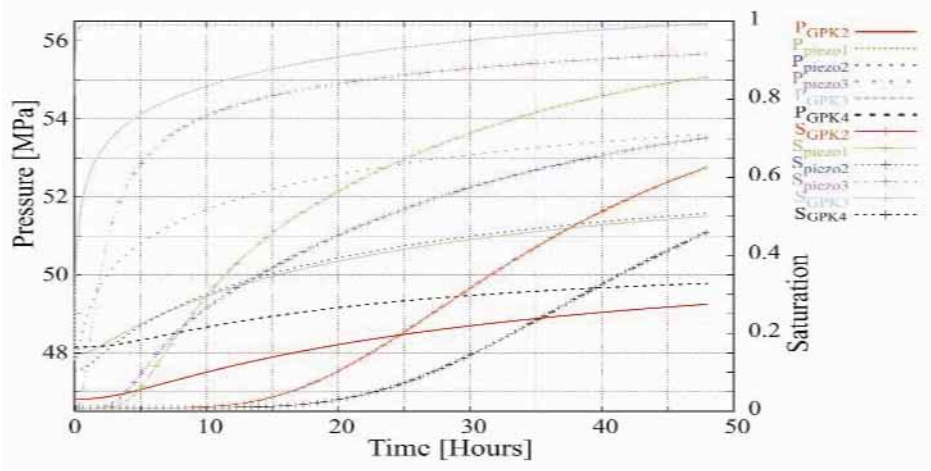

Figure 10. Calculated pressure and saturation for the first simulation.

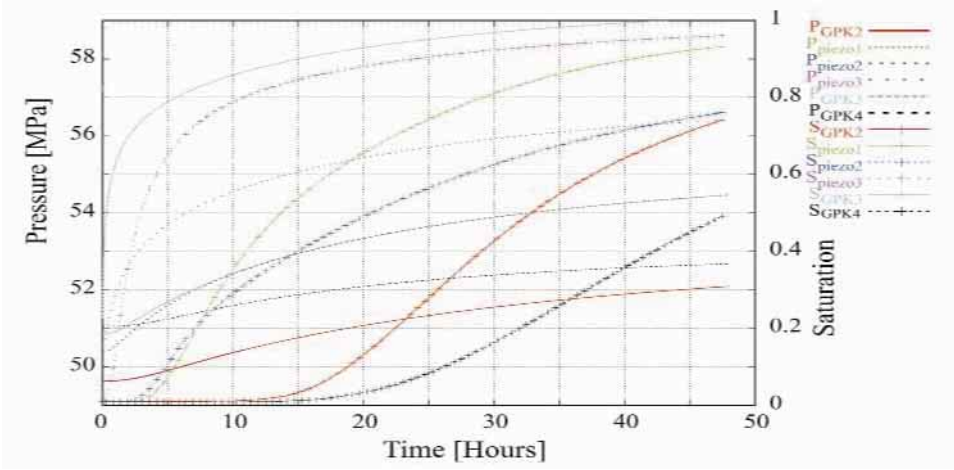

Figure 11. Calculated pressure and saturation for the second simulation.

Conclusion

The numerical code we propose has demonstrated that it is a reasonably efficient tool for simulating two phase flow in fractured zone. Verifications are performed against various examples that are solved in the litterature. One of the interesting points of this program is that we can start from homogeneous isotropic systems and continue with more heterogeneous fracture networks. These kinds of networks would be very practical and useful to study and predict the behaviour of anisotropic fractured media.

From a numerical point of view, the IMPES resolution scheme gives acceptable results in terms of accuracy and computing time, even if the time step used has to be limited in order to obtain a good convergence of the solver.

The main objective of our work is now to account for temperature exchanges be tween fluids and rock matrix in order to take into account eventual density and viscosity changes for both fluids. This work is of prior importance to understand long term hydraulic experiences. Simulating long term tests with a small contrast of density and short term tests with a higher contrast helps us in defining alternative stimulation strategies using fluid of high density and should leed us to enhance actual results obtained in the simulation of the Soultz-sous-Forets heat exchanger.

References

BANDIS, S., A. LUMSDEN, and N. BARTON, (1960). Fundamentals of rock joints deformatione flow. *Int. J. Rock Mech. Min. Sci. and Geomech. Abstr.* 20(5), 852-864.

BRUEL, D., (2003). Stratégie de développement par stimulation d'un systeme multipuits et caractérisation hydraulique du réservoir développé. Technical report, GEIE/Armines Research contract ref::N•G069/02-1305.

BUCKLEY, S. E. and M. C. LEVERETT, (1946). Mechanism of fluid displacement in sands. *Trans. AIME* 146, 107-116.

CACAS, M., (1989). *Développement d'un modele tridimensionnel stochastique discret pour la simulation de l'écoulement et des transferts de masse et de chaleur en milieu fracturé.* Ph. D. thesis, Ecole Nationale Supérieure des Mines de Paris.

COATS, K. H., (2000). A note on impes and impes-based simulation models. *Society of Petroleum Engineers September,* 245-251.

DAHLE, H., M. ESPEDAL, R. EWING, and O. SAEVAREID, (1990). Characteristics adaptative subdomain methods for reservoir flow problems. *Numerical Methods for Partial Differential Equations* 6, 279-309.

FAUST, C. R., (1985). Transport of immiscible fluids within and below the unsaturated zone: A numerical model. *Water Resources Research* 21 (4), 587-596.

FORSYTH, P., A. UNGER, and E. SUDICKY, (1997). Nonlinear methods for nonequilibrium multiphase subsurface flow. *Advances in Wat. Res.* 21, 433-489.

GENTIER, S., (1986). *Morphologie et comportement hydromécanique d'une fracture naturelle dans un granite sous contrainte normale.* Ph. D. thesis, Université d'Orléans.

HELMIG, R., (1997). *Multiphase flow and transport processes in the subsurface.* Springer Verlag.

HUYAKORN, P., S. PANDAY, and Y. YU, (1994). A three dimensional multiphase flow model for assessing napl contamination in porous and fractured media, 1. formulation. *Journal of Gontaminant Hydrology* 16(2), 109-130.

HUYAKORN, P. and G. PINDER, (1983). *Gomputational methods in subsurface flow.* Academic Press.

HUYAKORN, P. and G. F. PINDER, (1978). A new finite element technique for the solution of two-phase flow trough porous mediand fractured media. *Advances in Wat. Res.* 1(16), 285-298.

JEONG, W., (2000). *Modélisation de l'influence d'une zone de failles sur l'hydrogéologied'un milieu fracturé: application au domaine du stockage des déchets nucléaires.* Ph. D. thesis, Ecole Nationale Supérieure des Mines de Paris.

MARSILY, G. D., (1981). *Hydrogéologie quantitative.* Masson.

PEACEMAN, D. W., (1977). *Fundamentals of numerical reservoir simulation.* Elsevier.

SETTARI, A. and K. AZIZ, (1990). *Petroleum reservoir simulation.* Elsevier applied science.

SLOUGH, K., E. SUDICKY, and P. FORSYTH, (1999). Numerical simulation of multiphase flow and phase partitionning in discretely fractured media. *Journal of Contaminant Hydrology 40,107*-136.

THORENZ, C., (2001). *Model adaptative Simulation of Multiphase and Density Driven Flow in Fractured and Porous Media.* Ph. D. thesis, Universität Hannover.